Agricultural and Forest Meteorology 308-309 (2021) 108537

Contents lists available at ScienceDirect

Agricultural and Forest Meteorology

journal homepage: www.elsevier.com/locate/agrformet

Cover crop residue moisture content controls diurnal variations in surface residue decomposition

Resham Thapa [a,b,*], Katherine L Tully [a], Miguel Cabrera [c], Carson Dann [c], Harry H. Schomberg [b], Dennis Timlin [d], Julia Gaskin [c], Chris Reberg-Horton [e], Steven B. Mirsky [b]

[a] Department of Plant Science and Landscape Architecture, University of Maryland-College Park, MD, USA 20742.
[b] Sustainable Agricultural Systems Laboratory, USDA-ARS, Beltsville Agricultural Research Center, Beltsville, MD, USA 20705.
[c] Department of Crop and Soil Sciences, University of Georgia, Athens, GA, USA 30602.
[d] Adaptive Cropping Systems Laboratory, USDA-ARS, Beltsville Agricultural Research Center, Beltsville, MD, USA 20705.
[e] Department of Crop and Soil Sciences, North Carolina State University, Raleigh, NC, USA 27695.

ARTICLE INFO

Keywords:
Cover crops
Residue water retention properties
Residue decomposition
Diurnal variations
No-till systems

ABSTRACT

The effect of cover crop (CC) surface residues on water, carbon, and nitrogen cycling in no-till systems depends in part on the water retention properties of decomposing residues and the extent of decomposition. This study (1) examined the effect of decomposition on residue water retention properties; (2) characterized diurnal variations in residue decomposition rates in response to changes in soil-residue-air environmental conditions; and (3) examined the diurnal relationships between cover crop surface residue decomposition and residue environment (moisture and temperature). Maximum gravimetric water content (θ_g) and characteristic water release curves were determined for red clover (*Trifolium pratense* L.) and cereal rye (*Secale cereale* L.) residues collected at 0, 4, 10, and 16 weeks after termination for red clover, and at 2, 5, and 18 weeks for cereal rye. In addition, residue carbon dioxide (CO_2-C) flux, along with soil-residue-air environmental conditions, were measured diurnally for red clover at 4, 10, and 16 weeks after termination, and for cereal rye at 5 weeks after termination. Maximum residue θ_g decreased as decomposition progressed. Cover crop residue decomposition also influenced water release curves such that the water retained at any given water potential ($\psi_{residue}$) declined with increasing decomposition. These decomposition-associated changes in residue water retention properties were strongly related to residue lignin concentrations. Cover crop surface residue CO_2-C flux showed distinct diurnal patterns that were strongly related to $\psi_{residue}$ or residue θ_g. At a diurnal scale, residue CO_2-C flux increased during the nighttime from 18:00 to 06:00 h when residues gain moisture from the atmosphere and soil, and decreased during the daytime from 06:00 to 18:00 h when residues lost moisture via evaporation. Increase in temperature decreased residue CO_2-C flux due to moisture limitations. Therefore, CC surface residue decomposition models must address both diurnal changes in $\psi_{residue}$ and the changes in water retention properties as residues decompose.

1. Introduction

In the mid-Atlantic US states, cover crop (CC) based no-till grain production systems are widely promoted and incentivized to reduce nutrient and sediment loading into the Chesapeake Bay Watershed (*Mirsky et al., 2012*; *NRC, 2011*; *Thapa et al., 2018a*; *Wallace et al., 2017*). In these systems, CC residues are retained at the soil surface as a mulch and provide multiple ecosystem services, some of which include soil and moisture conservation, weed suppression, and nutrient cycling (*Mirsky et al., 2012*). The effect of surface residues on the underlying soil environment has been widely studied. Cover crop surface residues act as a physical barrier and protect soil from sealing and crusting by rainfall, conserve soil moisture during dry periods via reduced evaporation, decrease light transmittance, and moderate surface soil temperature fluctuations (*Bristow, 1988*; *Teasdale and Mohler, 1993*). The extent to which CC surface residues affect soil physical environment depends on

Abbreviations: CC, cover crops; $\psi_{residue}$, residue water potential; ψ_{air}, air water potential θ_g, gravimetric water contents; RH, relative humidity; NIRS, near infra-red reflectance spectroscopy.

* Corresponding author.
E-mail addresses: rthapa@umd.edu, reshambt1@gmail.com (R. Thapa).

https://doi.org/10.1016/j.agrformet.2021.108537
Received 2 August 2020; Received in revised form 21 March 2021; Accepted 29 June 2021
Available online 14 July 2021

the mass, thickness, and quality of the surface residue layer, which in turn drives decomposition (*Dietrich et al., 2019; Poffenbarger et al., 2015*). Therefore, understanding processes and drivers of surface residue decomposition is critical for developing effective residue management strategies in no-till systems.

Surface residue decomposition is strongly influenced by residue environmental conditions such as moisture (θ_g) and temperature (*Quemada and Cabrera, 1997; Stott et al., 1986; Thapa, 2021*). The surface residue layer is directly exposed to solar radiation, wind, dew, and rainfall under field conditions. Hence, environmental conditions (θ_g and temperature) in the residue layer can change more dramatically and dynamically than in the underlying soil layers, which will likely result in temporal heterogeneity in the decomposition of surface residues. While soil θ_g and temperature is simple to measure and can be easily obtained from weather stations, continuous measurement or monitoring of θ_g and temperature in a CC surface residue layer is difficult. As a result, to our knowledge there are no field studies that measured diurnal variations in surface residue environmental conditions (θ_g and temperature) and their effect on decomposition in agricultural systems. Studies in temperate forest ecosystems have suggested that diurnal variations in the decomposition of forest floor litter samples tracked variations in air temperature (*Jomura et al., 2012; Witkamp, 1969; Zimmermann et al., 2009*). However, these studies were conducted in the cold and wet winter months (September - November) under dense forest canopies; findings from forest ecosystems may be of limited use in CC-based no-till cropping systems in which decomposition of CC residues typically occurs during the hot and dry summer months. Therefore, it is critical to understand how θ_g and temperature in the CC residue layer change diurnally and how these changes drive decomposition.

Crop residues can store a significant amount of water depending on residue quantity and the frequency, intensity, and duration of rainfall or irrigation (*Kozak et al., 2007; Savabi and Stott, 1994; Scopel et al., 2004*). The maximum amount of water retained by undecomposed crop residues differs among crop species (*Iqbal et al., 2013; Quemada and Cabrera, 2002; Savabi and Stott, 1994*). Few studies have attempted to develop mathematical relationships to determine the water retention capability of crop residues based on residue characteristics (*Iqbal et al., 2013; Quemada and Cabrera, 2002*). Previous studies found that the maximum water retentive capacity of undecomposed crop residues is highly correlated to soluble carbohydrate concentrations (i.e. chemical characteristics) (*Quemada and Cabrera, 2002*) or tissue density of the crop residues (i.e. physical characteristics) (*Iqbal et al., 2013*). Since crop residues undergo physical and chemical transformations during decomposition, the maximum water retention capacity of the crop residues will most likely change over time. Moreover, the degree to which residue particles have decomposed may affect the evolution of residue θ_g during the evaporation period following rainfall or irrigation events. Hence, the degree of decomposition may alter the residue θ_g and water potential ($\psi_{residue}$) relationships. Although it is evident that the absorption or desorption of θ_g from crop residues during wetting and drying periods is largely regulated by water retention properties, there is currently a knowledge gap on the decomposition associated changes in CC residue water retention properties.

This study aimed to address existing knowledge gaps by (1) determining the effect of decomposition on the water retention properties of CC residues, (2) characterizing diurnal variations in residue decomposition and soil-residue-air environmental conditions in no-till systems, and (3) examining the diurnal relationships between residue decomposition and residue environment (moisture and temperature) in no-till systems.

2. Materials and methods

2.1. Experimental site and management

This study was conducted in the Cover Crop Systems Project (CCSP), a long-term agricultural research (LTAR) site that is part of the USDA-ARS LTAR network, located at the Beltsville Agricultural Research Center (39°00′51.3"N, 76°56′29.0"W, Beltsville, MD, US). Soil at the experimental site was classified as Codorus (fine-loamy, mixed, active, mesic Fluvaquentic Dystrudepts) and Hatboro (fine-loamy, mixed, active, nonacid, mesic Fluvaquentic Endoaquepts) soil series with a silt loam texture (*Soil Survey Staff, 2020*). We selected two experimental plots from a conventionally-managed continuous no-till system in a corn (*Zea mays* L.)-soybean (*Glycine max* L.)-winter wheat (*Triticum aestivum* L.) rotation. Red clover (*Trifolium pratense* L.) was seeded into winter wheat at the rate of 17 kg ha^{-1} on March 16, 2018 using a no-till drill. Cereal rye (*Secale cereale* L.) was drill-seeded at the rate of 134 kg ha^{-1} on October 24, 2018 following corn harvest. Red clover was terminated at the anthesis stage on May 8, 2019 using a mixture of 0.84 kg ha^{-1} glyphosate (N-(phosphonomethyl) glycine)) 0.42 kg ha^{-1} dicamba (3,6-dichloro-2-methoxybenzoic acid), and 0.28 kg ha^{-1} 2,4-D (2,4-Dichlorophenoxyacetic acid). Similarly, cereal rye was terminated at the heading stage on May 9, 2019 using a mixture of 1.26 kg ha^{-1} glyphosate, 0.35 kg ha^{-1} glory (Metribuzin), and 1.49 kg ha^{-1} Dual II Magnum (S-metolachlor). Cover crop residues were left intact on the surface as a mulch following termination. Soybean was planted green into the preceding cereal rye CC using a no-till drill on May 8, 2019; corn was drilled into the red clover mulch on May 17, 2019.

2.2. Study periods and cover crop (CC) characterization

We performed a series of diurnal experiments to understand how surface residues at various stages of decomposition respond to changes in environmental conditions. Decomposition of red clover residues was measured at 4, 10, and 16 weeks after termination, which corresponded to corn growth stage of V1-V2, tasseling, and R6 stage, respectively. Similarly, cereal rye decomposition was measured at five weeks after termination, at the soybean V2 growth stage. During each study period, residue and soil θ_g, $\psi_{residue}$, residue, soil, and air temperatures, and air relative humidity (RH) were also measured (see below in Section 2.4 for more details). In addition to these diurnal study periods, CC residue samples were collected at week 0 (red clover), week 2 (cereal rye), and week 18 (cereal rye) and analyzed for maximum residue θ_g; water release curves were then generated following the procedure as described in Section 2.3.

Residue sub-samples from each sampling event were air-dried, finely ground to pass through 1-mm sieve, and sent to the Agriculture and Environmental Services Labs at the University of Georgia (Athens, GA) for quality analysis. Percent carbohydrate, cellulose, hemicellulose, and lignin in the residue samples were determined via near infra-red reflectance spectroscopy (NIRS) using scanning monochrometer (model 6500; FOSS NIRSystems, Silver Spring, MD). Total C and N concentrations in the CC residues were determined by dry combustion using a Leco TruMac CN Analyzer (LECO Corporation, St. Joseph, MI).

2.3. Determination of maximum residue water content and characteristic water release curves

To investigate the impact of residue decomposition on water retentive capacity, we determined the maximum residue θ_g at various stages of decomposition (red clover: 0, 4, 10, and 16 weeks after termination; cereal rye: 2, 5, and 18 weeks after termination). The maximum residue θ_g was calculated following the procedure outlined by Quemada and Cabrera *(2002)*. In brief, CC residues were cut into $\leq$0.5 cm pieces, immersed in distilled water overnight, and then drained to remove

excess water. Triplicate samples of drained residue samples were weighed before and after oven-drying at 60°C for 48 h. The maximum residue θ_g was finally expressed on an oven-dried weight basis.

We also investigated the impact of residue decomposition on characteristic water release curves for both red clover and cereal rye residues. Moisture release or water retention curves provide the relationship between $\psi_{residue}$ and residue θ_g. Residue collected from diurnal experiments was used to determine the water release curves of red clover (weeks 4, 10, and 16) and cereal rye residues (week 5). For other sampling events (red clover residues collected at week 0 and cereal rye residues collected at weeks 2 and 18), the water release curves were determined following the procedure described by Quemada and Cabrera (2002). The water-saturated pieces of residue samples (handled as described above) were spread on trays and allowed to air-dry under ambient room conditions. At various hours during the drying process, residue sub-samples were transferred to round sampling cups to measure $\psi_{residue}$ using a WP4C Dewpoint Potentiometer (METER Group, Inc., Pullman, WA). The residue cups were weighed immediately and then oven-dried at 60°C for 2 d to determine residue θ_g.

2.4. Diurnal measurements of residue decomposition and soil-residue-air environmental conditions

Diurnal variations in red clover and cereal rye decomposition rates were determined by measuring residue CO_2-C flux at approximately 0:00, 6:00, 9:00, 12:00, 15:00, 18:00, and 21:00 hours. The CO_2-C flux from red clover residues was measured at 4 (June 3-5, 2019), 10 (July 18-20, 2019), and 16 (August 29-31, 2019) weeks after termination. Based on a companion litter bag decomposition study conducted on the same study site, the estimated biomass of red clover residues during June, July and August study periods were 704, 453, and 340 g m^{-2}, respectively. Similarly, the CO_2-C flux from cereal rye residues was measured at five (Jun. 14-16, 2019) weeks after termination (estimated biomass based on a companion litter bag decomposition study was 536 g m^{-2}). No rain fall during any of these study periods. However, the experimental plots received variable amounts of rain on the day prior to the start of each study period (1.78, 11.9, 3.30, and 0.25 mm of rain on June 2, June 13, July 17, and August 28, respectively).

Residue CO_2-C flux (g m^{-2} hr^{-1}) was measured in the field using a portable EGM-4 infrared gas analyzer system (PP Systems, Amesbury, MA) equipped with a flow-through closed SRC-2 Soil Respiration Chamber (PP Systems, Amesbury, MA). The chamber had a volume of 1171 cm^3 and a surface area of 78 cm^2. At the time of CO_2-C flux measurements, CC residues from an equivalent area (~78 cm^2) were cut and transferred to a beaker. The chamber tops were placed on beakers and sealed perfectly to measure CO_2-C flux from residues within 300 sec. This method was preferred because it excluded soil-derived CO_2-C flux and allowed us to capture the actual decomposition rates of surface CC residues in no-till systems. Following CO_2-C flux measurements, CC residues were transferred into plastic zippered bags, sealed, and brought back to the laboratory to measure $\psi_{residue}$ and residue θ_g within 1-2 h. In addition, we collected surface soil samples (0-5 cm depth, 2-cm diameter probe) from the same place where the residue samples were taken for CO_2-C flux measurements. Measurements (residue and soil θ_g, $\psi_{residue}$, and residue CO_2-C flux) were repeated on four different samples.

In the laboratory, residue samples were cut into ≤0.5 cm pieces and the $\psi_{residue}$ was measured using a WP4C Dewpoint Potentiometer. The residue cups were then weighed immediately and oven-dried at 60°C for 2 d to determine residue θ_g. The $\psi_{residue}$ and residue θ_g were determined in triplicate sub-samples per replicate. Therefore, we had 12 values of $\psi_{residue}$ and residue θ_g for each measurement hour. To determine soil θ_g, surface soil samples were weighed before and after oven-drying at 104°C for 2 d.

During each study period, air temperature and RH was monitored at 75 cm above the soil surface using a T9602-3-D-1 Humidity & Temperature Probe Sensor (Amphenol Advanced Sensors, Mansfield, TX) and recorded at 10 min intervals using a customized Arduino-based datalogger. A 107-Temperature Probe Sensor (Campbell Scientific, Inc., Logan, UT) was inserted inside the CC mulch layer to measure residue temperature. Soil temperature and volumetric moisture content (θ_g) were measured by installing a time-domain reflectometer TDR-310S probe sensor (Acclima, Inc., Meridian, ID) at a 45° angle beneath the residue layer. Surface CC residue temperature, soil temperature, and soil θ_g were recorded at 10 min intervals using a CR1000 datalogger (Campbell Scientific, Inc., Logan, UT). Air water potential (ψ_{air}) was calculated from air temperature and RH data using the following equation:

$$\psi_{air} = \frac{R \cdot T}{V} \cdot \frac{ln(RH) \cdot 1\ MPa}{1,000,000\ Pa} \quad (1)$$

where R is the universal gas constant (8.314 J K^{-1} mol^{-1}), T is the absolute air temperature (K), V is the partial molar volume of water (1.8 × 10^{-5} m^3 mol^{-1}), and RH is the air relative humidity expressed as a fraction (0-1).

2.5. Data analysis

Characteristic moisture release curves for each CC residue (red clover or cereal rye) at different stages of decomposition were fitted using the *nls* function in R. The basic form of the characteristic moisture release curve can be presented as follows:

$$\psi_{residue} = a \cdot (residue\ \theta_g)^{-b} \quad (2)$$

where $\psi_{residue}$ is the residue water potential (MPa), θ_g is the gravimetric moisture content of the residue (g water g^{-1} dry residue), and '*a*' and '*b*' are empirical constants of the model. The '*a*' represents the plateau of the moisture release curve (estimated maximum residue θ_g) and '*b*' represents the shape of the moisture release curve (propensity of the residue to lose moisture as it dries, i.e. as $\psi_{residue}$ decreases). Simple linear regression was performed using *lm* function in R to examine if the maximum residue θ_g and the characteristic moisture release curves could be estimated based on residue chemical characteristics; the best fit parameters are presented in subsequent figures.

Linear and non-linear regression models were fitted to examine the relationship between residue CO_2-C flux and environmental variables for each study period independently. Data points where residue CO_2-C flux was equal to zero were excluded during analysis to avoid overfitting of the model equations. Separate regression models were determined for each study period. To determine if residue type and the extent of decomposition affected the relationship between CC residue θ_g and CO_2-C flux, the slopes and intercepts of the linear models were compared using the *emmeans* package in R (Lenth, 2019).

3. Results

3.1. Residue chemistry changes during decomposition

As CC residue decomposition progressed, residue N concentrations increased, thus leading to lower C:N ratios over time (Table 1). The chemical characteristics of the CC surface residues also changed during decomposition. The percentage of carbohydrate in the red clover tissue decreased initially from week 0 to 4, while the proportion of cellulose and hemi-cellulose increased during the same period (Table 1). At later stages of decomposition, i.e. from week 4 to 16, carbohydrate and cellulose concentrations in the red clover tissue remained nearly constant. Hemi-cellulose concentrations in the remaining red clover residues slightly decreased from week 4 to 16. In a similar manner, hemi-cellulose concentrations in the remaining cereal rye residues also decreased over time. Conversely, the lignin concentrations increased

Table 1
Biochemical characteristics of red clover and cereal rye residues at various stages of decomposition in 2019.

Residue	Study period	C %	N	C:N ratio	Carbohydrate %	Cellulose	Hemi-cellulose	Lignin
Red clover	May (0 week)	43.2	2.58	16.8	50.8	29.9	8.8	5.6
Red clover	June (4 week)	42.3	2.61	16.2	33.5	37.4	12.6	10.2
Red clover	July (10 week)	43.8	2.89	15.2	32.2	37.9	12.0	12.7
Red clover	August (16 week)	43.3	3.02	14.3	34.0	36.3	10.2	13.9
Cereal rye	May (2 week)	43.8	0.96	45.5	21.6	38.6	30.7	7.4
Cereal rye	June (5 week)	44.9	0.99	45.2	22.4	43.0	26.2	9.0
Cereal rye	September (18 week)	45.2	1.19	38.0	24.8	44.2	20.9	11.3

over time; the relative increase was greater for red clover than cereal rye. We found a quadratic relationship between lignin concentrations and time (red clover: $y = -0.04x^2 + 1.12x + 5.78$, $R^2 = 0.99$ and cereal rye: $y = -0.02x^2 + 0.71x + 6.03$, $R^2 = 1$).

3.2. Changes in residue water retention properties during decomposition were linked to changes in residue lignin concentrations

The maximum water retentive capacity of the CC residues decreased as decomposition progressed (Fig. 1). The maximum θ_g of the red clover and cereal rye residues decreased by 53.1% (from week 0 to 16) and 15.7% (from week 2 to 18), respectively. Irrespective of the CC species and decomposition stage, the power function presented in equation [2] adequately fitted the relationship between $\psi_{residue}$ and residue θ_g (Fig. 1; $R^2 = 0.80$ - 0.99). We observed differences among the moisture release curves of red clover residues sampled at weeks 0, 4, and 10 (Fig. 1a). However, red clover residues sampled at weeks 10 and 16 showed no differences among the moisture release curves. As decomposition progressed, the water retained by red clover residues declined at high $\psi_{residue}$ (> -30.0 MPa). More water was retained by undecomposed (week 0) residues, followed by slightly-decomposed (week 4) residues, and then by moderately-to-highly decomposed red clover residues (weeks 10 and 16). At a very negative $\psi_{residue}$ (< -30.0 MPa), the residue θ_g was quite similar between decomposed and undecomposed red clover residues. Cereal rye residue decomposition and water retentive capacity followed the same pattern as that of red clover (Fig. 1b). At a given $\psi_{residue}$, the highest θ_g was found in the least decomposed cereal rye residues (week 2) and the lowest θ_g in the highly decomposed cereal rye residues (week 18). Cereal rye residues collected at week 5 had intermediate values of residue θ_g.

Decomposition-associated changes in residue water retention properties were directly linked to changes in residue chemical characteristics. We found that the maximum residue θ_g decreased linearly with increasing residue lignin concentrations (Fig. 2a). Similarly, parameter '*a*' of the characteristic moisture release curve also decreased linearly with the increase in residue lignin concentrations (Fig. 2b). Conversely, parameter '*b*' of the characteristic moisture release curve increased linearly with the increase in residue lignin concentrations (Fig. 2c). These results indicate a common set of equations for both red clover and cereal rye residues can be used to predict maximum residue θ_g and parameters '*a*' and '*b*' of the characteristic moisture release curves.

3.3. Diurnal variations in surface residue decomposition: Effect of residue moisture and temperature

Air, residue, and soil temperatures exhibited similar diurnal patterns such that they increased between 06:00 and 16:00 h and decreased between 16:00 and 06:00 h on each day (Figs. 3, 4). The amplitudes of the diurnal patterns also varied substantially between study periods. We observed greater diurnal fluctuations in the temperature of surface residues than surface soils. Residue temperature consistently increased to values higher than soil temperature during daytime and decreased to values similar to or lower than soil temperature during nighttime.

The diurnal patterns of ψ_{air} followed the patterns of air RH (Figs. 3, 4). Similarly, the diurnal patterns of the $\psi_{residue}$ followed the diurnal patterns of ψ_{air} such that the maximum values of the $\psi_{residue}$ were observed early in the morning at 06:00 h and then sharply decreased to reach daily minimums at 15:00 h. These patterns were completely opposite to those observed for soil, residue, and air temperatures. In addition, $\psi_{residue}$ had more extreme diurnal fluctuations during June than July or August. During June, the $\psi_{residue}$ of red clover fluctuated between -0.95 and -147.6 MPa while that of cereal rye fluctuated between -0.08 and -118.5 MPa (Figs. 3a, 4). The $\psi_{residue}$ of red clover fluctuated between -5.15 and -68.4 MPa during July and between -2.36 and -73.7 MPa during August (Figs. 3b, c).

Diurnal patterns of the residue θ_g were similar to those of $\psi_{residue}$(Figs. 3, 4). The maximum values of the residue θ_g (red clover:

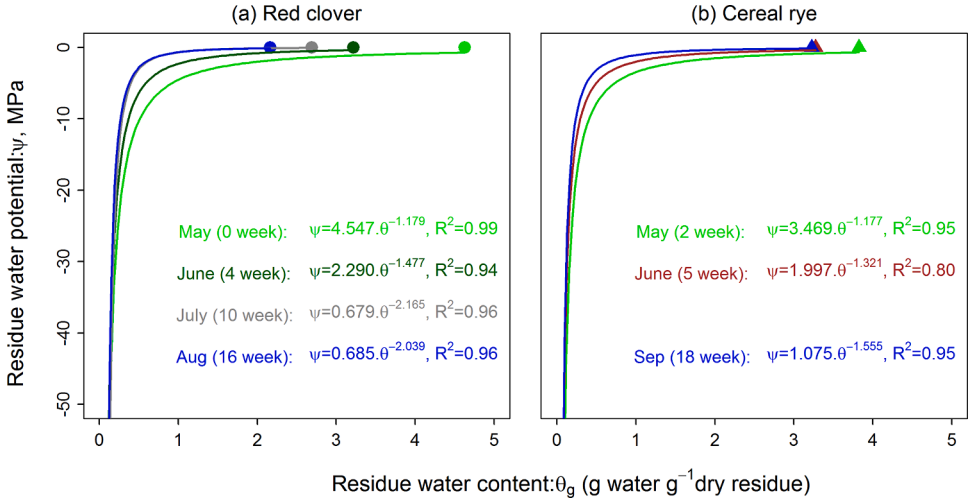

Fig. 1. Characteristic moisture release curves for (a) red clover [n=49 (May); n=179 (June); n=180 (July); n=135 (Aug)] and (b) cereal rye [n=64 (May); n=121 (June); n=40 (Sep)] residues at various stages of decomposition in 2019. 'n' represents the number of points used for fitting the moisture release curves. The curves were fitted using the power function presented in equation [2] and the fitted equations were presented in subsequent figures. Solid points in the figures represent the actual maximum residue water content as determined in the laboratory. For clarity purposes, other points, indicating residue water potential values for corresponding gravimetric water contents, are not shown in the graphs.

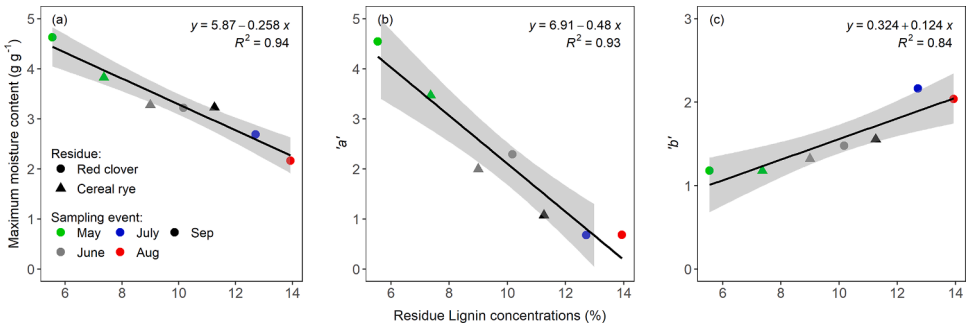

Fig. 2. Water retention properties of decomposing cover crop residues as a function of residue lignin concentrations: (a) maximum residue moisture content, (b) parameter '*a*' of the characteristic moisture release curves, and (c) parameter '*b*' of the characteristic moisture release curves. The equation of the linear models and their corresponding R^2 values are presented. Grey bands represent the 95% confidence interval of the modeled lines.

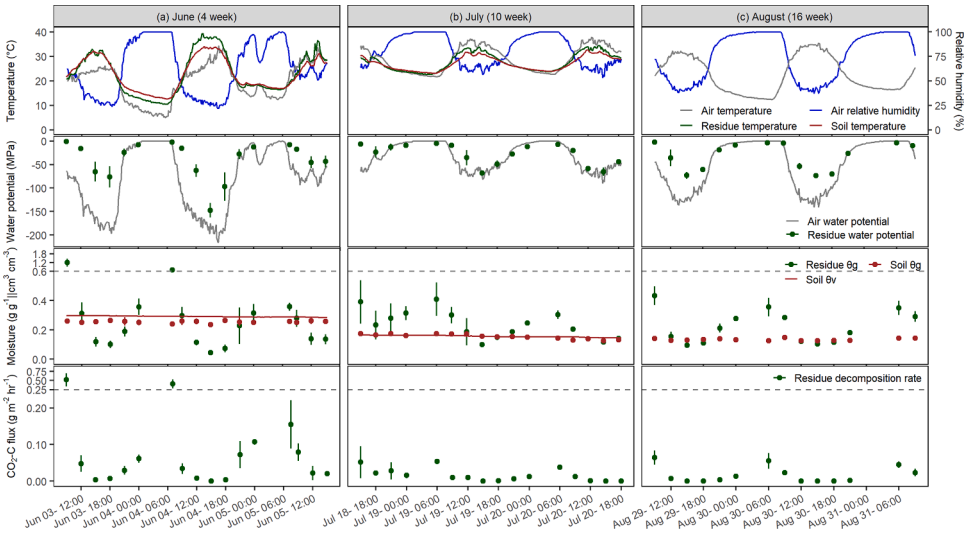

Fig. 3. Diurnal variations in red clover residue decomposition rate (CO_2-C flux) and soil-residue-air environmental conditions for the (a) June (4 weeks after termination), (b) July (10 weeks after termination), and (c) August (16 weeks after termination) study periods in 2019. Residue CO_2-C flux, residue and soil gravimetric moisture content (θ_g), and residue water potential ($\psi_{residue}$) were measured at approximately 0:00, 6:00, 9:00, 12:00, 15:00, 18:00, and 21:00 hours each day. Air relative humidity (RH), soil-residue-air temperatures, and soil volumetric moisture content (θ_v) were continuously monitored at 10 min intervals throughout the study duration. Dashed lines indicate change in Y-axis scale for moisture and CO_2-C flux graphs.

0.30 - 1.20 g g^{-1}; cereal rye: 0.37 - 2.58 g g^{-1}) were observed at 06:00 h on each day. After 06:00, residue θ_g sharply decreased during the daytime to reach its daily minimum values of 0.05 - 0.14 g g^{-1} for red clover and 0.04 - 0.07 g g^{-1} for cereal rye at 15:00 h. After 15:00, residue θ_g gradually increased during the nighttime. Conversely, surface soil θ_g and θ_v did not show diurnal variations and remained relatively constant throughout each study period.

Across all study periods, residue CO_2-C flux also showed diurnal fluctuations such that they decreased sharply between 06:00 and 12:00 h (morning), exhibited very little or undetectable CO_2-C flux between 12:00 and 18:00 h (daytime), and gradually increased between 18:00 and 06:00 h (afternoon and nighttime; Figs. 3, 4). The amplitudes of the diurnal patterns were observed at 06:00 h on each day; amplitudes decreased from one day to the next. For example, the peak CO_2-C flux from red clover residues during Jun. 3-5, 2019 decreased from 0.518 to 0.408 g m^{-2} hr^{-1} on day 1, down to 0.155 g m^{-2} hr^{-1} on day 2 (Fig. 3a). Similarly, the peak CO_2-C flux from cereal rye residues decreased from 0.197 at day 0 to 0.085 to 0.072 g m^{-2} hr^{-1} on days 1 and 2, respectively (Fig. 4). Similar observations were made during July and August study periods, though magnitudes were smaller. Diurnal variations in residue CO_2-C flux strongly tracked diurnal variations in $\psi_{residue}$ and residue θ_g.

Residue CO_2-C flux increased exponentially with the $\psi_{residue}$, while a positive linear relationship was found between residue CO_2-C flux and residue θ_g (Fig. 5). Conversely, residue CO_2-C flux decreased with increasing temperature (Fig. 6). We also examined the effect of residue type and the extent of decomposition on moisture sensitivity of surface residue decomposition. The slopes and intercepts of the linear models (residue CO_2-C flux *vs.* residue θ_g) were significantly higher for red clover compared to cereal rye (Table 2). To examine the effect of the extent of decomposition on moisture sensitivity of residue decomposition, data from red clover residues were compared between three study periods (June, July, and August). Although the intercepts of the linear models did not vary between these study periods, the slope was significantly higher for June compared to July and August (Table 2). The slopes for July and August study periods were not significantly different.

4. Discussion

4.1. Residue chemistry changes during decomposition

Cover crop residues differ greatly in their chemical composition, which in turn will affect their decomposition rate under given soil and climatic conditions (*Cabrera et al., 2005*; *Poffenbarger et al., 2015*; *Thapa et al., 2018b*). Several studies have suggested that residue constituents sequentially decompose such that carbohydrates are degraded before holo-cellulose (cellulose + hemi-cellulose) and holo-cellulose before lignin (*Gunnarsson et al., 2008*; *Gunnarsson and Marstorp 2002*, *Harman et al., 2008F*). Studies have also suggested the occurrence of simultaneous decomposition of residue constituents, with the rate of decomposition decreasing in the following order: carbohydrate > holo-cellulose > lignin (*Woodruff et al., 2018*). Nonetheless, differences in the time and rate of decomposition of residue constituents will change the chemical composition of the remaining residues during decomposition.

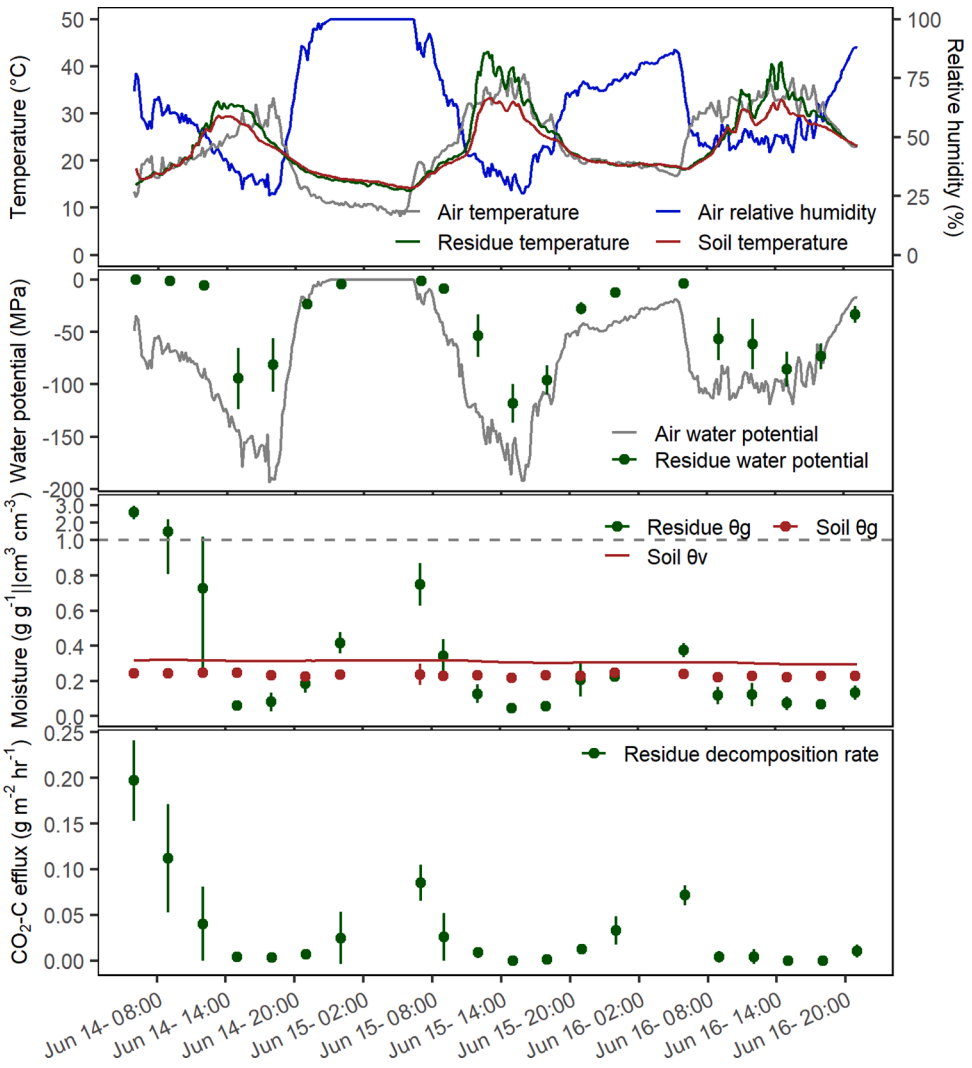

Fig. 4. Diurnal variations in cereal rye residue decomposition rate (CO_2-C flux) and soil-residue-air environmental conditions during the June 14-16, 2019 (5 weeks after termination) study period. Residue CO_2-C flux, residue and soil gravimetric moisture content (θ_g), and residue water potential ($\psi_{residue}$) were measured at 0:00, 6:00, 9:00, 12:00, 15:00, 18:00, and 21:00 hours each day. Air relative humidity (RH), soil-residue-air temperatures, and soil volumetric moisture content (θ_v) were continuously monitored at 10 min intervals throughout the study duration. Dashed lines indicate change in Y-axis scale for moisture and CO_2-C flux graphs.

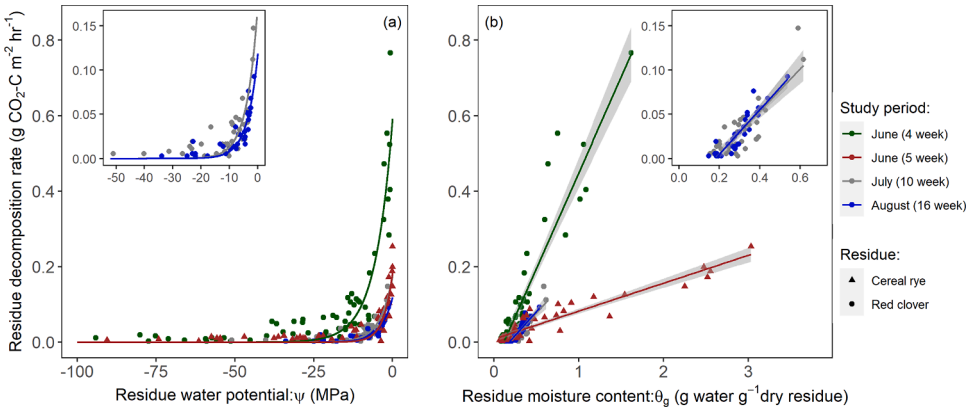

Fig. 5. Relationship between surface residue decomposition rate (CO_2-C flux) and (a) residue water potential ($\psi_{residue}$), and (b) residue moisture content (θ_g) for each study period in 2019. Different colors represent different study periods; different shapes represent different cover crop residue types. Note that measurements where CO_2-C flux was equal to zero were excluded during analysis. Parameters of the model fits are presented in Table 2. Grey bands represent 95% confidence intervals.

In this study, we observed a sharp decrease in the carbohydrate concentration of red clover tissue until week 4, perhaps due to faster decomposition of readily decomposable carbohydrate fractions (Table 1). This concomitantly increased cellulose and hemi-cellulose concentrations in the red clover residue. Although hemi-cellulose concentrations initially increased, they started to decrease at later stages of decomposition for both red clover and cereal rye residues. In contrast, residue lignin concentrations increased over time, probably due to the intense degradation of carbohydrate and holo-cellulose fractions and the resultant increase in the recalcitrant lignin fractions via microbial by-

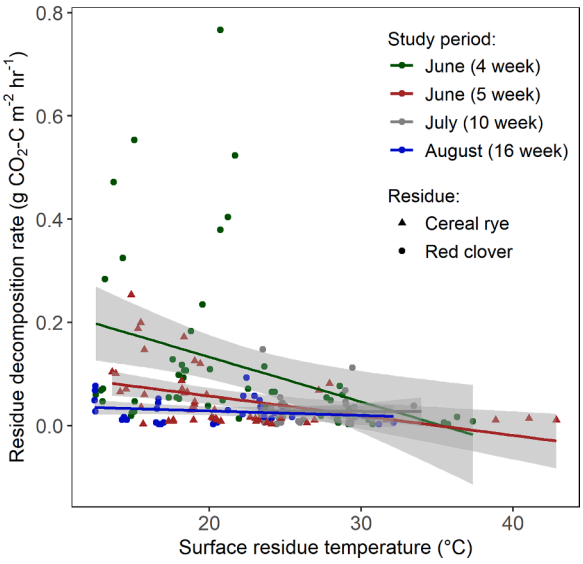

Fig. 6. Relationship between surface residue decomposition rate (CO_2-C flux) and residue temperature for each study period in 2019. The decrease in surface residue CO_2-C flux with increasing residue temperature was due to decrease in moisture availability for microorganisms in the surface residue layers as temperature increases in no-till fields. Different colors represent different study periods; different shapes represent different cover crop residue types. Due to the failure of a data logger, we used air temperature at 75 cm height instead of residue temperature for the August study period. Note that measurements where CO_2-C flux was equal to zero were excluded during analysis. Grey bands represent 95% confidence intervals.

products during decomposition. Our results are consistent with many previous studies that have also found that decomposing crop residue lignin concentrations increased over time (*Gao et al., 2016*; *Harman et al., 2008*; *Jahanzad et al., 2016*; *Kriauciuniene et al., 2008*).

Changes in the physical characteristics of CC residues were not evaluated in this study. However, studies have suggested that the decomposition of cellulose and hemi-celluloses leads to the formation of macropores within decomposed tissues (*Iqbal et al., 2013*; *Maloney and Paulapuro, 1999*). This loss of cellular components over time would alter the pore size distribution such that the decomposed residues have an increase in macropores. Such changes in the physical and chemical characteristics of CC residues during decomposition would strongly influence water retention properties, which impacts not only decomposability, but also water exchange processes between soil-residue-air interfaces.

4.2. Changes in residue water retention properties during decomposition were linked to changes in residue lignin concentrations

We observed that the maximum residue θ_g decreased with increasing decomposition for both CC species (Table 1). In sharp contrast, Iqbal et al. *(2013)* found that the decomposition of maize stems increased residue water retentive capacity and suggested that the increase in maximum θ_g was due to an increase in porosity during decomposition. Differences between these studies could be explained by the distinct morphological characteristics of the maize stems. Maize stems are characterized by the presence of pith (the inner, sponge-like porous material) and bark (the outer, hard envelope). Since water is mostly stored in pith within maize stems, it may be possible that the increase in the volume of macropores during decomposition allowed pith to absorb more water in decomposed maize stems (*Iqbal et al., 2013*). However, CC residues used in this study were devoid of pith and hence, the water molecules may have been preferentially stored in the cell walls of decomposing tissues as bound water. Water molecules are bound or adsorbed to OH groups present in cellulose, hemi-cellulose, and lignin by the H-bonding force (*Jiang et al., 2019*). Jiang et al. *(2019)* further suggested that the availability of OH groups increased with increasing cellulose and hemi-cellulose fractions and decreased with increasing lignin fractions in the cell wall. Therefore, the changes in water retention properties of the decomposing CC residues likely may have been due to decomposition-associated changes in the residue chemical characteristics. Supporting this hypothesis, we found that the maximum θ_g that residues can hold decreased linearly with increasing lignin concentrations in the decomposing CC residues (Fig. 2a).

The characteristic moisture release curves of the CC residues were also strongly influenced by the extent of decomposition (Fig. 1). At any given $\psi_{residue}$, the θ_g of both red clover and cereal rye residues decreased as residue decomposed. In other words, residue θ_g of the decomposed residues dropped sharply even with a slight decline in $\psi_{residue}$, which was probably due to the presence of large volumes of macropores. In this study, we found that the decomposition-associated changes in characteristic moisture release curves can be best predicted as a function of residue lignin concentrations (Fig. 2b, c). Given that the lignin concentrations in the CC residues can be quickly and easily determined using near infra-red spectroscopy (NIRS) technique, we propose the use of lignin as a proxy for water retention properties (maximum residue θ_g and parameters '*a*' and '*b*' of the moisture release curves) of the decomposing CC residues. From a modelling perspective, defining decomposition-associated changes in the characteristic moisture release curves (parameters '*a*' and '*b*') is highly critical because it helps us determine existing water potential gradients and hence, the rate at which is transferred among soil-residue-air interfaces under a given environmental condition (Dann et al. unpublished).

4.3. Diurnal variations in surface residue decomposition: Effect of residue moisture and temperature

Surface CC residues can influence the soil physical environment in no-till cropping systems. Residue acts as a physical barrier that intercepts solar radiation and thus reduces the maximum soil temperature (*Bristow, 1988*; *Teasdale and Mohler, 1993*). Consistent with previous studies, we found that the residue layer experienced greater temperature extremes than the underlying surface soil in the daytime (Fig. 3, 4). The

Table 2
Parameters of regression models fitted between residue decomposition rate (CO_2-C flux) and (a) residue water potential ($\psi_{residue}$) and (b) residue moisture content (θ_g) for each study period in 2019. Residue CO_2-C flux was exponentially related to $\psi_{residue}$ and linearly related to residue θ_g.

Residue	Study period	(a) Residue water potential $CO_2 - C\ flux = a \cdot exp^{(b \cdot \psi_{residue})}$			(b) Residue moisture content† $CO_2 - C\ flux = m \cdot \theta_g + c$		
		a	b	R^2	slope (m)	Intercept (c)	R^2
Red clover	June (4 week)	0.5917	0.1827	0.85	0.5078 Aa	-0.0594 aA	0.86
Red clover	July (10 week)	0.1751	0.2584	0.75	0.2405 b	-0.0429 a	0.70
Red clover	August (16 week)	0.1181	0.2679	0.84	0.2513 b	-0.0453 a	0.83
Cereal rye	June (5 week)	0.1838	0.3531	0.83	0.0741 B	0.0080 B	0.89

† Different lowercase letters within a column represent significant differences between study periods for red clover residue. Different uppercase letters within a column represent significant differences between red clover and cereal rye residues for June study period. Significant differences were determined at $p<0.05$.

maximum temperature in the CC residue layer and surface soil differed by as much as 2.2 to 10°C. During nighttime, both soil and residue temperature declines and the rate of cooling of residue layers can be sometimes faster than that of surface soils (Fig. 3, 4). For instance, the temperature in the red clover residue layer was 2.1°C lower than that in surface soil during early June. Therefore, CC residues experienced greater diurnal fluctuations in temperature than surface soils.

Our study further highlights that CC residues experience extreme diurnal fluctuations in residue θ_g or $\psi_{residue}$ and hence, undergo frequent dry-wet cycles: the residue θ_g declines below soil θ_g during the day (extreme drying) and rises above soil θ_g during the night (wetting) (Fig. 3, 4). The condensation of water vapor into dew, resulting from cool nights and high humidities at the study site, led to water absorption by CC residues during the nighttime. The underlying residue layer that is in contact with the soil can also serve as a sponge for water absorption from moist soil surfaces (*Kutlu et al., 2018*). The effect of soil water content on residue water content likely increased as decomposition progressed due to increase in soil-residue contact. As the sun rises, the water is rapidly lost to the atmosphere from CC residues via evaporation. The rate at which water is gained or lost from CC residues depends on the water potential gradient among soil-residue-air interfaces, which in turn is regulated by air temperature, RH, and soil moisture (Dann et al., *in prep.*). Although not quantified, we noticed that the topmost residue layer gained or lost water more rapidly compared to the underlying residue layer that is in direct contact with the soil. Therefore, depending on the residue thickness, a vertical moisture gradient exists such that different residue layers may decompose at different rates in the field.

To our knowledge, there is no study that measured diurnal variations in surface residue decomposition in no-till cropping systems. For the first time, we found that residue decomposition in no-till cropping systems exhibits distinct diurnal patterns that are strongly related to residue θ_g or $\psi_{residue}$ (Fig. 3, 4). Residue CO_2-C fluxes were typically observed during the nighttime, when residues gained moisture from the atmosphere (Fig. 3, 4). Depending on CC species and the extent of decomposition, residue θ_g or $\psi_{residue}$ explained 70-89% of the diurnal variations in residue decomposition rate (Fig. 5a, b; Table 2). Decomposition of red clover residues was more sensitive to residue θ_g than cereal rye residues. This suggests that CC residues of a recalcitrant nature (high C:N ratio and lower carbohydrate fractions) decompose more slowly under the given environmental conditions. Moreover, we observed that the moisture-sensitivity of residue decomposition decreased as decomposition progressed. The slopes of a linear model (CO_2-C flux vs residue θ_g for red clover) were significantly higher in June as compared to the July and August 2019 study periods (Table 2). Initial decomposition (in June) reduced the amount of readily decomposable material available for each successive measurement period. In addition, residue quantity decreased over time, resulting in significantly lower CO_2-C flux (g m^{-2} hr^{-1}) during late-stage of decomposition. Another factor may be decomposition-associated changes in residue water retention properties, as discussed earlier.

Although the positive response of residue decomposition to temperature has been frequently reported in laboratory incubation studies (*Quemada and Cabrera, 1997; Stott et al., 1986*), residue decomposition decreased with increasing temperature under field conditions (Fig. 6). This was because the increase in residue temperature resulted in the decrease of residue θ_g or $\psi_{residue}$ to values that substantially limited microbial decomposition of CC residues (Figs. 3, 4). Based on these findings, we can conclude that the decomposition of CC residues in no-till fields is strongly moisture-limited on dry days.

5. Conclusions

This study, to our knowledge, provides the first *in-situ* evidence that the water retention properties of CC residues change during decomposition in response to changes in residue physical (e.g., porosity) and chemical characteristics. As decomposition of CC residues progressed over time, the maximum residue θ_g decreased. Characteristic moisture release curves of the CC residues were also strongly influenced by decomposition such that the propensity of the residues to lose moisture (decrease in residue θ_g relative to decrease in $\psi_{residue}$) increased with increasing decomposition. Results further suggest that the water retention properties (maximum residue θ_g, as well as the parameters '*a*' and '*b*' of the characteristic moisture release curves) of the CC residues at any stage of decomposition can be determined based on lignin concentrations in the decomposing residues.

In addition, this study demonstrated that CC residues in no-till fields experienced extreme diurnal fluctuations in moisture (θ_g or $\psi_{residue}$) and temperature compared to underlying soils. Surface residue decomposition also showed distinct diurnal patterns that were strongly coupled to residue moisture. Increases in residue temperature, however, decreased residue decomposition because microbial activity was limited by moisture at elevated temperatures under field conditions. Based on these findings, we can conclude that the decomposition of CC residues in no-till fields is strongly controlled by residue moisture, which in turn depends on environmental conditions and the water retention properties of CC residues. Therefore, accurate simulation of surface residue decomposition in no-till fields will require mechanistic models that can accurately predict residue moisture based on information easily available from weather stations.

Declaration of Competing Interest

The authors declare that they have no known competing financial interests or personal relationships that could have appeared to influence the work reported in this paper.

Acknowledgments

This work was supported by the Northeast Sustainable Agriculture Research and Education (SARE) graduate student grant (award # GNE17-160-31064) awarded to Resham Thapa and the USDA Natural Resources Conservation Services (Conservation Innovation Grant # 8042-21660-004-36-R). We express our sincere thanks to the technical staff of the Sustainable Agricultural Systems Laboratory, USDA-ARS, Beltsville Agricultural Research Center, Beltsville, MD for managing the long-term cover crop systems project. We would also like to acknowledge Dr. Jude Maul for providing the EGM-4 infrared gas analyzer system, Alondra Thompson for providing the data logger system used in this experiment, and Dr. Victoria Ackroyd for proof-reading the manuscript.

Supplementary materials

Supplementary material associated with this article can be found, in the online version, at doi:10.1016/j.agrformet.2021.108537.

References

Bristow, K.L., 1988. The role of mulch and its architecture in modifying soil temperature. Aust. J. Soil Res. 26, 269–280.

Cabrera, M.L., Kissel, D.E., Vigil, M.F., 2005. Nitrogen mineralization from organic residues: research opportunities. J. Environ. Qual. 34, 75–79.

Dietrich, G., Recous, S., Pinheiro, P.L., Weiler, D.A., Schu, A.L., Rambo, M.R.L., Giacomini, S.J., 2019. Gradient of decomposition in sugarcane mulches of various thickness. Soil Tillage Res. 19, 66–75.

Gao, H., Chen, X., Wei, J., Zhang, Y., Zhang, L., Chang, J., Thompson, M.L., 2016. Decomposition dynamics and changes in chemical composition of wheat straw residue under anaerobic and aerobic conditions. PLoS One 11 (7), e0158172 doi: 10.1371/journal. Pone.0158172.

Gunnarsson, S., Marstorp, H., 2002. Carbohydrate composition of plant materials determines N mineralisation. Nutr. Cycl. Agroecosyst. 62, 175–183. https://doi.org/10.1023/A:1015512106336.

Gunnarsson, S., Marstorp, H., Dahlin, A.S., Witter, E., 2008. Influence of non-cellulose structural carbohydrate composition on plant material decomposition in soil. Biol. Fertil. Soils 45, 27–36 doi 10.1007/s00374-008-0303-5.

Harman, J., Moorhead, D., Berg, B., 2008. The relationship between rates of lignin and cellulose decay in aboveground forest litter. Soil Biol. Biochem. 40 (10), 2620–2626.
Iqbal., A., Beaugrand, J., Garnier, P., Recous, S., 2013. Tissue density determines the water storage characteristics of crop residues. Plant Soil 367, 285–299. https://doi.org/10.1007/s11104-012-1460-8.
Jahanzad, E., Barker, A.V., Hashemi, M., Eaton, T., Sadeghpour, A., Weis, S.A., 2016. Nitrogen release dynamics and decomposition of buried and surface cover crop residues. Agron. J. 108 (4), 1735–1741. https://doi.org/10.2134/agronj2016.01.0001.
Jiang., Y., Lawrence, M., Hussain, A., Ansell, M., Walker, P., 2019. Comparative moisture and heat sorption properties of fibre and shiv derived from hemp and flax. Cellulose 26, 823–843. https://doi.org/10.1007/s10570-018-2145-0.
Jomura, M., Kominami, Y., Ataka, M., 2012. Differences between coarse woody debris and leaf litter in the response of heterotrophic respiration to rainfall events. J. Forest Res. 17 (3), 305–311.
Kozak, J.A., Ahuja, L.R., Green, T.R., Ma, L., 2007. Modelling crop canopy and residue rainfall interception effects on soil hydrological components for semi-arid agriculture. Hydrol. Processes 21, 229–241.
Kriauciuniene, Z., Velicka, R., Raudonius, S., Rimkeviciene, M., 2008. Changes of lignin concentration and C: N in oilseed rape, wheat and clover residues during their decomposition in the soil. Agronomy Res. 6 (2), 489–498.
Kutlu, T., Guber, A.K., Rivers, M.L., Kravchenko, A.N., 2018. Moisture absorption by plant residue in soil. Geoderma 316, 47–55. https://doi.org/10.1016/j.geoderma.2017.11.043.
Lenth, R., 2019. emmeans: Estimated Marginal Means, aka Least-Squares Means. R package version 1.4.2. https://CRAN.R-project.org/package=emmeans.
Maloney, T.C., Paulapuro, H., 1999. The formation of pores in the cell wall. J. Pulp Paper Sci. 25, 430–436.
Mirsky, S.B., Ryan, M.R., Curran, W.S., Teasdale, J.R., Maul, J., Spargo, J.T., Moyer, J., Grantham, A.M., Weber, D., Way, T.R., Camargo, G.G., 2012. Conservation tillage issues: Cover crop-based organic rotational no-till grain production in the mid-Atlantic region, USA. Renew. Agricult. Food Syst. 27 (1), 31–40. https://doi.org/10.1017/S1742170511000457.
National Research Council, 2011. Achieving Nutrient and Sediment Reduction Goals in the Chesapeake Bay: An Evaluation of Program Strategies and Implementation. The National Academies Press, Washington, DC, USA.
Poffenbarger, H.J., Mirsky, S.B., Weil, R.R., Kramer, M., Spargo, J.T., Cavigelli, M.A., 2015. Legume proportion, poultry litter, and tillage effects on cover crop decomposition. Agron. J. 107 (6), 2083–2096. https://doi.org/10.2134/agronj15.0065.
Quemada, M., Cabrera, M.L., 1997. Temperature and moisture effects on C and N mineralization from surface applied clover residue. Plant Soil 189, 127–137.
Quemada, M., Cabrera, M.L., 2002. Characteristic moisture curves and maximum water content of two crop residues. Plant Soil 238, 295–299.
Savabi, M.R., Stott, D.E., 1994. Plant residue impact on rainfall interception. ASAE Paper 92–2634.
Scopel, E., Da Silva, F.A.M., Corbeels, M., Affholder, F., Maraux, F., 2004. Modelling crop residue mulching effects on water use and production of maize under semi-arid and humid tropical conditions. Agronomie 24, 383–395. https://doi.org/10.1051/agro:2004029.
Stott, D.E., Elliott, L.F., Papendick, R.I., Campbell, G.S., 1986. Low temperature or low water effects on microbial decomposition of wheat residue. Soil Biol. Biochem. 18 (6), 577–582.
Teasdale, J.R., Mohler, C.L., 1993. Light transmittance, soil temperature, and soil moisture under residue of hairy vetch and rye. Agron. J. 85, 673–680.
Thapa, R., Tully K.L., Cabrera M.L., Dann C., Schomberg H.H., Timlin D., Reberg-Horton C., Gaskin J., Davis B.W., Mirsky S.B.,, 2021. Effects of moisture and temperature on C and N mineralization from surface-applied cover crop residues. Biology and Fertility of Soils 57 (4), 485–498. https://doi.org/10.1007/s00374-021-01543-7.
Thapa, R., Mirsky, S.B., Tully, K.L., 2018a. Cover crops reduce nitrate leaching in agroecosystems:A global metaanalysis. J. Environ. Qual. 47 (6), 1400–1411. https://doi.org/10.2134/jeq2018.03.0107.
Thapa, R., Poffenbarger, H., Tully, K.L., Ackroyd, V., Kramer, M., Mirsky, S.B., 2018b. Biomass production and nitrogen accumulation by hairy vetch-cereal rye mixtures: a meta-analysis. Agron. J. 110, 1197–1208 https://doi.org/10.2134/agronj2017.09.054.
Wallace, J.M., Williams, A., Liebert, J.A., Ackroyd, V.J., Vann, R.A., Curran, W.S., Keene, C.L., VanGessel, M.J., Ryan, M.R., Mirsky, S.B., 2017. Cover Crop-Based, Organic Rotational No-Till Corn and Soybean Production Systems in the Mid-Atlantic United States. Agriculture 7 (4), 34. https://doi.org/10.3390/agriculture7040034.
Witcamp, M., 1969. Cycles of temperature and carbon dioxide evolution from litter and soil. Ecology 50 (5), 922–924.
Woodruff, L.K., Kissel, D.E., Cabrera, M.L., Hitchcock, R., Gaskin, J., Vigil, M., Sonon, L., Saha, U., Habteselassie, M.Y., Rema., J., 2018. A web-based model of N mineralization from cover crop residue decomposition. Soil Sci. Soc. Am. J. 82, 983–993.
Zimmermann, M., Meir, P., Bird, M., Malhi, Y., Ccahuana, A., 2009. Litter contribution to diurnal and annual soil respiration in a tropical montane cloud forest. Soil Biol. Biochem. 41, 1338–1340.